Green Edge Directed Demosaicing Algorithm

H. Phelippeau, H. Talbot, M. Akil, S. Bara

Abstract— *In recent years, digital cameras have become the dominant image capturing devices. They are now commonly included in other digital devices such as mobile phones and PDAs, and have become steadily cheaper, more complex and powerful. In such devices, in order to keep costs down, only incomplete color information is recorded at each pixel location. Interpolating a full three-color image by estimating the missing component is called demosaicing. Clearly, the quality of this reconstruction is of crucial importance for the overall image quality experienced by the end-user. It influences sharpening perception, texture details, grain, color artifacts, signal to noise ratio and processing time. Hand-held devices suffer from inefficient demosaicing induced by their power limitations and their architectural constraints. In this paper we propose a new demosaicing algorithm delivering high image quality while keeping a computational complexity compatible with hand-held devices. Images quality and computational complexity are compared to the state of the art. An implementation of our algorithm on a common multimedia processor is presented and highlights the real time performance of our proposed algorithm*[1].

Index Terms — photography, single sensor devices, imaging.

I. INTRODUCTION

Digital cameras are now commonly included in many digital devices such as mobile phones, PDAs, and are becoming steadily cheaper, more complex and powerful. In such devices, a single CCD (Charge Coupled Device) or CMOS (Complementary Metal Oxide Semiconductor) sensor is used to convert incident light into electric signal (see Fig. 1). Both CCD and CMOS sensors do not significantly differentiate light wavelengths during photons counting and are consequently color insensitive. To introduce color sensitivity, a color filter array, made up with the three additive primary colors (red, green, and blue) mosaic is superimposed on the sensor. Several mosaic schemes have been proposed, the most popular has been proposed by Bayer in [1], as shown on Fig. 1. The Bayer mosaic uses twice as many green elements as red or blue in an attempt to mimic the human eye's greater sensibility to green light. Thus, the sensor gets solely one-third of color information coming from the scene image, the remaining two-thirds have to be estimated to produce a full color image. This is done with a demosaicing algorithm. This step is of crucial importance for image quality. It influences sharpening, structure details, grain, color artifacts, signal to noise ratio and processing time. Since the emergence of hand-held single sensor devices, industry showed much interest towards this subject, and many demosaicing algorithms have been proposed, requiring various amounts of computing power and providing various levels of image quality. Recent and thorough literature overviews are presented in [2]-[3]-[4]. Demosaicing can be applied during normal camera processing operations or offline for cameras capable of producing raw data. In common compact devices, raw data is not available to end-users, who only have access to images after they have been processed by the camera's internal logic units. When choosing the demosaicing algorithm for embedded solution, one needs to consider devices architecture and power limitations as well. This generally leads to the use of low-complexity algorithms, associated with relatively weak image quality, instead of more powerful solutions available.

In this paper, we propose a new demosaicing algorithm, which we call GEDI (for Green Edge Directed Interpolation) delivering best-of-class image quality, while keeping a computational complexity compatible with hand-held camera devices. The paper is organized as follow; in section II, we present the main digital photography imaging pipeline; in section III, we present the problem of demosaicing and the state of the art; in section IV we present a novel edge directions estimator, GED (for Green Edge Direction); in section V, we propose a method for correcting wrong estimation directions, which we call LMDC (for Local Majority Direction Choice); in section VI we present a new way to reduce demosaicing color artifacts using the bilateral filter; in section VII we resume the GEDI demosaicing algorithms steps, in VIII and IX, we compare both produced image quality and computational complexity of GEDI to the most used literature algorithms; in section X we exhibit the real-time performance of GEDI on a current DSP[2].

II. DIGITAL PHOTOGRAPHY IMAGING OVERVIEW

As Costantini shows in [5], a digital image is the result of three main steps, let's see the general block diagram of a common digital photography system in Fig. 1. First, the optical image is formed through the lenses system, it includes main control devices, such as automatic gain control (AGC), auto focus and auto exposure circuitry. Then, the light signal is converted into electric current trough the digital sensor, including analog to digital conversion (ADC). Finally, the digital step is completed with digital image processing operations trough the embedded architecture, including demosaicing, white balance, noise removal, contrast, brightness and gamma adaptations, etc. The output image is sent to the baseband for storage or to the interface for visualization. Demosaicing appears usually as the first image

[1] H.Phelippeau, H.Talbot, M.Akil are with the Université de Paris Est, LabInfo, Institut Gaspard Monge, Groupe ESIEE, 93162, Noisy le Grand Cedex France (e-mail: phelipph, talboth, akilm@esiee.fr).

H.Phelippeau, S.Bara are with the NXP Semiconductors, 2 esplanade Anton Philips, Campus effiscience, Colombelles, BP 2000, 14906 Caen Cedex 9, France (e-mail: harold.phelippeau, stefan.bara@nxp.com).

[2] TM3270 from the NXP semiconductors TriMedia DSP family

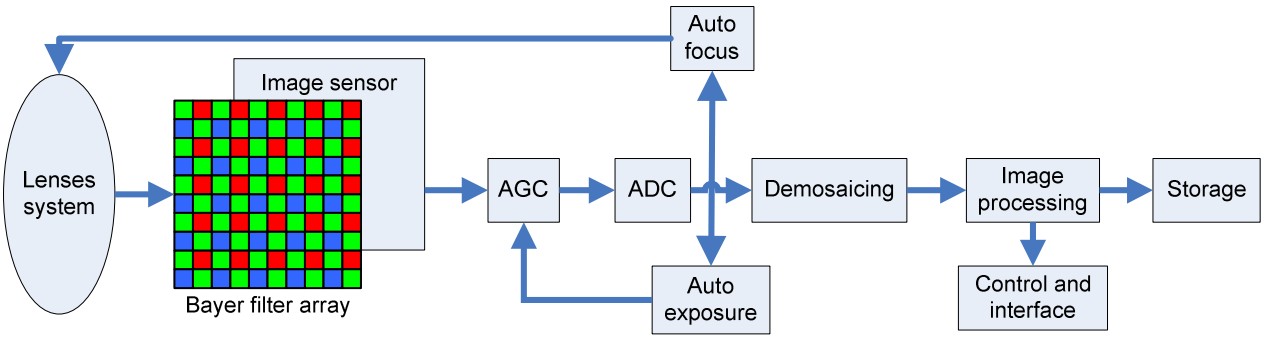

Fig. 1 . General block diagram of a digital camera system.

processing task, occurring immediately after sensor output. It determines the input image quality of the processing chain and is of crucial importance for the output image quality. In the following section we present the literature related to demosaicing algorithms.

III. INTRODUCTION TO DEMOSAICING

Since the 1980s, many research works were proposed regarding Bayer mosaic interpolation, from simple to advanced methods [2]-[3]-[4]. In this section, we present non-exhaustively the main demosaicing algorithm principles.

Generally, because of its better resolution, the green channel is interpolated first, the red and blue channels are deduced from it. An efficient way to interpolate red and blue channels from the green one is the Constant Hue Interpolation (CHI) method, proposed by Cok in [6]. The intuitive idea is that hue information varies little across an object surface. It follows that for an *(R,G,B)* color vector, the ratios *R/G*, *B/G* varies slowly in a real image. In spite of the non-linear sensors response, the channels differences $R_{-}=(R-G)$ and $B_{-}=(B-G)$ also varies slowly in a digital photography image. Following this idea, the CHI algorithm is performed in four steps: (1) interpolate the green channel; (2) calculate the difference channels R_{-} and B_{-} at red and blue filters locations; (3) bilinearly interpolate R_{-} and B_{-} channels (as from Cock's assumption, hue contains few high spatial frequencies, and the bilinear interpolation does not induce significant loss of information); (4) add the green channel to the interpolated difference channels R_{-} and B_{-} to compute the red and blue output channels. Using this method, the high spatial frequencie informations of the green channel are injected in the red and the blue channels. Various algorithms use this technique, for instance [7]-[8]-[9]-[10]-[11]-[12]-[13]-[14].

The most basic idea to estimate the missing green components is to use the bilinear interpolation, which exhibits many defects such as blur, moiré and false colors, related to the Shannon-Nyquist limitation theorem. Improved isotropic interpolation algorithms have been developed using optimal weights, based on mean square error minimization, as propose Crane in [15] and Malvar in [16]. In spite of their ability to reduce bilinear defects, such algorithms do not deliver sufficient image quality because of their lack of dependence to the image content.

In [7], Kimmel proposes an adaptive weighted average algorithm considering local image details. The weights are calculated as the photometric dependence of the bilateral filter proposed by Tomasi in [17]. The same approach is used by Ramanath in [18]. This approach reduces blur and moiré effects significantly. However, it needs to be iterated several times to yield effective color artifacts reduction. Moreover, the weights calculation is a source of important computational complexity.

Another idea is to interpolate missing color components following details directions, consequently avoiding blur, moiré and color artifacts simultaneously. Based on the fact that the visual world is mainly composed of horizontal and vertical directions, it was demonstrated that, using an efficient details directions estimator, an excellent image quality could be produce using solely these two basics interpolation directions (see [2]-[3]-[8]). Various details directions estimators have been proposed in the literature. In [9], Hibbard proposes to compare vertical and horizontal green gradients. In [19], Laroche compares red and blue second order gradients. Hamilton in [20] improves the estimator resolution by fusionning Hibbard and Prescott estimators. He also proposes to improve green pixels interpolations by reducing color artifacts and moiré effects, using red and blue correction terms as in (1). We use the notations of Fig. 2, where *G3* is the missing green pixel at the *R3* position.

$$G3 = \begin{cases} (G7+G8)/2 + (2R3 - R6 - R9)/4 \\ \textit{if the direction choice is horizontal} \\ (G2+G4)/2 + (2R3 - R1 - R5)/4 \\ \textit{if the direction choice is vertical} \end{cases} \quad (1)$$

In [8], Hirakawa proposes local homogeneity classifiers. This algorithm consists of interpolating full color image versions in both horizontal and vertical directions. Images are then converted from *RGB* to CIE*Lab* space. After color space conversion, local homogeneity maps are calculated using luminance and chrominance measures of closeness. Finally, the pixel value in either the vertical or horizontal interpolated image that exhibits the most homogeneous local neighborhood is chosen for the output image.

In [21], Alleyson proposes a new method for color demosaicing based on a mathematical model of spatial color multiplexing. He demonstrate that a one-color per pixel image

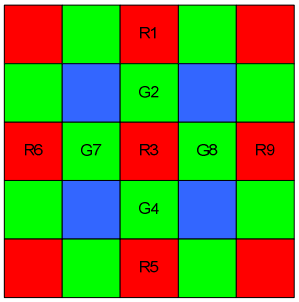

Fig. 2. Bayer matrix numbering.

can be written as the sum of luminance and chrominance. In case of a regular arrangement of colors, such as with the Bayer CFA, luminance and chrominance are well localized in the spatial frequency domain.

In [22], Gunturk, based on the work of Glotzbach in [23], proposes to take efficiently advantage of the existing inter-channel correlation, trought an alternating projections scheme. The algorithm forces similar high-frequencies characteristics on the green, red and blue channels.

Demosaicing could also be interpreted as an image formation inverse problem. Proposed algorithms account for the transformations performed by color filters, lens distortions, and sensor noise and determined the most likely output image, given the measured CFA image [4]-[24].

In this paper we propose a new demosaicing algorithm based on details directed interpolations. We propose a novel details directions estimator. This new estimator is coupled with a local majority direction choice algorithm that corrects possible wrong choices (interpreted as noise) by changing them to the local majority choice. Finally we propose a new algorithm to reduce color interpolation artifacts based on the bilateral filter [17].

IV. GREEN EDGE DIRECTED ESTIMATOR

Directed algorithms exhibit a good compromise between image quality and computational complexity. The popular method of Hamilton [20] and Hirakawa [8] share many similarities. Their only significant difference is in the way of estimating the interpolation direction. This difference determines their output image quality, which is proportional to their computational complexity. The quality varies from low to high as complexity varies in the same way. The first kind of algorithm is well adapted to hand-held devices but not the second. Taking as a starting point these two algorithms we seek to propose a new one, exhibiting the image quality achieved by Hirakawa while keeping a low computational complexity, allowing the association of high image quality demosaicing with handheld devices capabilities.

As it was discussed in section III, Hamilton proposes to perform gradient calculations on the Bayer mosaic to estimate interpolation directions while Hirakawa uses the full image color reconstruction with a complex selection criterion. We propose a new estimator based on gradient calculations in the green channel, we call it GED (for Green Edge Directed).

Consider $G_v(.)$ the vertical interpolated green channel and $G_h(.)$ the horizontal interpolated green channel, interpolated as Hamilton propose in [20], using the second order gradient correction terms described in section III. Consider the coordinates $(i,j) \in X$, where X is a set of *2-D* pixel positions and $G(.)$ is the output green channel. The GED estimator is expressed in (2), where $\Delta hG(i,j)$ and $\Delta hG(i,j)$ are respectively defined in (3) and (4).

$$G(i,j) = \begin{cases} G_h(i,j) \text{ if } \left[\nabla hG_h(i,j) + \nabla hG_v(i,j)\right] \\ \qquad\qquad \le \left[\nabla vG_h(i,j) + \nabla vG_v(i,j)\right] \\ G_v(i,j) \text{ otherwise} \end{cases} \quad (2)$$

$$\nabla hG(i,j) = \left|G(i-1,j) - G(i,j)\right| + \left|G(i+1,j) - G(i,j)\right| \quad (3)$$

$$\nabla vG(i,j) = \left|G(i,j-1) - G(i,j)\right| + \left|G(i,j+1) - G(i,j)\right| \quad (4)$$

Fig. 3b shows the sub-sampled Bayer sequence of image in Fig. 3a, selected to contain both horizontal and vertical features. Fig. 3c and Fig. 3d respectively shows the results of the green channel horizontal interpolation and the color output image after CHI. We observe that horizontal details are interpolated in the correct direction while vertical details are interpolated in the wrong direction, together with associated color artifacts. Fig. 3e and Fig. 3f respectively shows the results of the green channel vertical interpolation and the color output image after CHI. Conversely to the horizontal interpolation cases, the vertical details are interpolated effectively while the horizontal details are full of artifacts. Looking at Fig. 3 and using the preceding notations, Fig. 3c corresponds to $G_h(.)$ and Fig. 3e corresponds to $G_v(.)$. By looking at Fig. 3c and Fig. 3e we can consider that the horizontal interpolation cancels the vertical details and strengthens the horizontal details. Conversely the vertical interpolation cancels the horizontal details and strengthens the vertical details. Exploring this property we deduce the relation (5) for $(i,j) \in X$, where X is a vertical details area, and the relation (6) for $(i,j) \in X$, where X is an horizontal details area. Looking now at the classifier condition in (2) we see that this behavior allows us to choose the corresponding interpolation direction.

$$\left\{\nabla hG_h(i,j) \approx \nabla vG_h(i,j);\ \nabla vG_v(i,j) < \nabla hG_v(i,j)\right\} \quad (5)$$

$$\left\{\nabla vG_v(i,j) \approx \nabla hG_v(i,j);\ \nabla hG_h(i,j) < \nabla vG_h(i,j)\right\} \quad (6)$$

Due to classifiers limitations, closeness between image details and sensors resolution and noise perturbations, it is effectively impossible to avoid incorrect direction decisions, introducing color artifacts. In the following section, we propose an algorithm to estimate and correct interpolation directions.

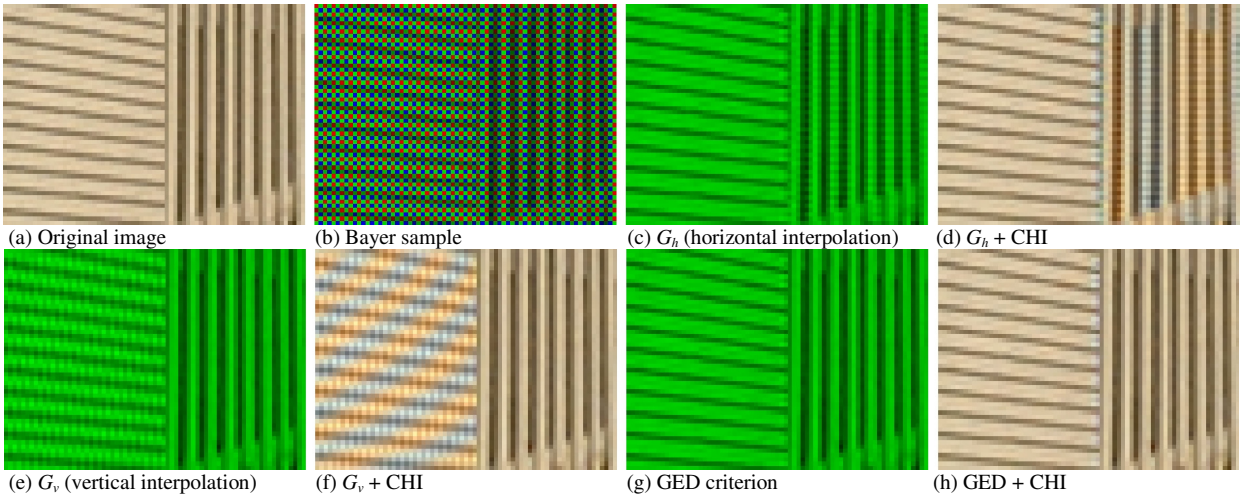

Fig. 3. Illustration of the GED classifier behavior.

V. Local Majoritary Direction Choice (LMDC) correction Method

Incorrect direction choices are introduced by classifiers precision weakness when using edge directed algorithms (see section III). These errors decrease image quality by introducing color artifacts and labyrinth-like structures. Examples are shown in Fig. 4b and Fig. 4f. We propose to estimate and correct these interpolation direction decisions by measuring the local majority direction choice (LMDC). If the direction choice of the current point is different to the LMDC, it is corrected to be homogeneous with its neighbors; else the original direction is kept. This method is based on the assumption that in real images details directions are continuous. If an interpolation direction is isolated, it is highly probable that this direction is false. The LMDC can be estimated using different window sizes and forms. Fig. 4 shows two examples of false interpolation correction using the LMDC method, while using Hamilton and Prescott demosaicing algorithms. Our proposal allows correcting an important number of false interpolations and increases the visual image quality by reducing color artifacts and labyrinth-like structures. Using a square window of size ($n \times n$) the complexity introduced in term of number of operations is (n^2+1) additions and 1 comparison per pixel, resulting in an improved image quality yet with a small complexity contribution. However, even with perfect interpolation direction choice there would be color artifacts inherent to interpolation. We now propose a new method for reducing such artifacts, based on the bilateral filter.

VI. Bilateral Artifacts Reduction Filter

Even a perfect demosaicing algorithm would yield color artifacts. These artifacts appear when image details are close to the sensor resolution. They are due to non-compliance with the conditions of the Nyquist-Shannon sampling theorem. A method to reduce color artifacts is proposed in [25], which consists of reducing color variations at an object surface by applying a median filter on the R_- and B_- difference channels. Generally, three iterations are necessary for effective artifacts reductions. Using a median function leads to a significant increase in algorithmic complexity, while limiting artifacts reductions due to the non convergence of the median filter. We show that better results can be obtained using adaptive mean weighted filters. In this section, we propose to study the filtering behavior of the mean and the bilateral filters [17] on the R_- and B_- difference planes. For the tests we used a square kernel of size (5×5). Fig. 5 shows visual results examples and comparisons between, median, mean and bilateral filters.

Fig. 5c, shows that the mean filter effectively erases color artifacts; however it also reduces color saturation. In Fig. 5g we observe that the mean filter spreads colors beyond the objects border (at the edge of the bloom). In contrast, as shown on Fig. 5d, the bilateral filter removes color artifacts better than the median filter. In Fig. 5h, the bilateral filter retains good color separations at object edges. We observe that the bilateral filter retains the good artifacts removing performances of the mean filter while keeping the objects edge separation property of the median filter. Table I shows the computational complexities of the studied algorithms. We conclude that using a bilateral filtering on the R_- and B_- difference planes increases the image quality while still keeping the computational complexity low.

TABLE I
ARTIFACTS REDUCTION ALGORITHMS COMPUTATIONAL COMPLEXITIES

Algorithms	Fixed Multiplications	Additions	Comparisons
Median n x n	0	$n^2 \times 2$	$n^2 + n \times 4$
Mean n x n	1	$n^2 - 1$	0
Bilateral n x n	$n^2 + 1$	$n^2 - 1$	0

VII. Complete Algorithm

Associating the local direction estimator GED with the LMDC correction, we prpose a new edge directed demosaicing algorithm wich we call GEDI for Green Edge Directed Interpolation. It is as follows.

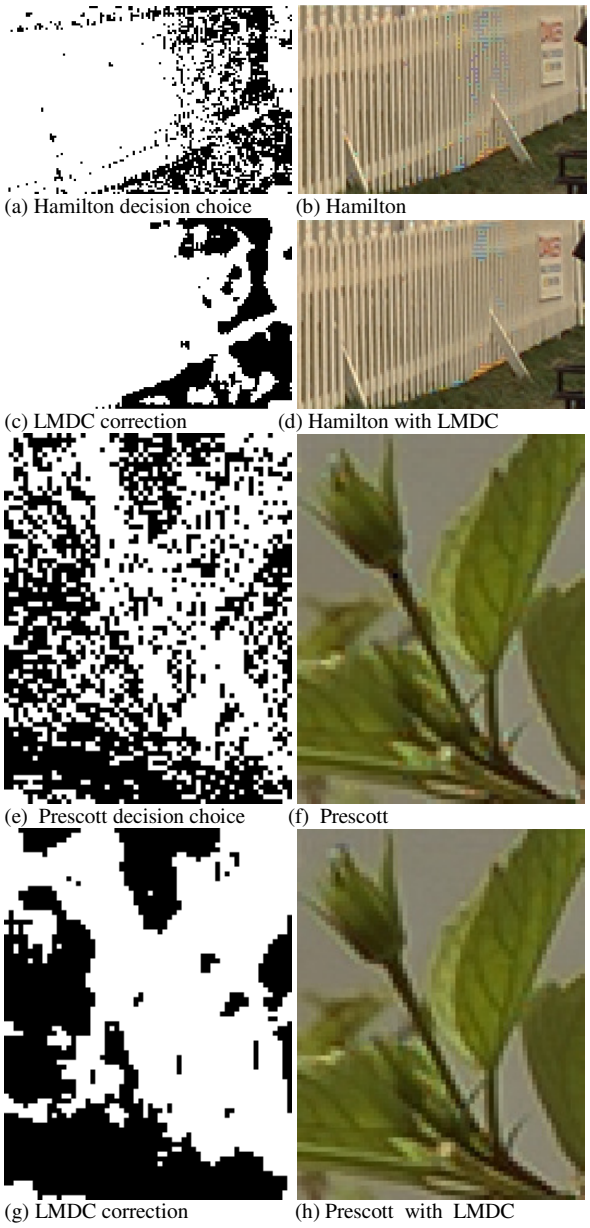

Fig. 4. Examples of results obtained with the LMDC method.

1) Horizontaly and verticaly interpolate the green channel using the second order gradient correction of the red and blue channels as proposes Hamilton in [20].
2) Estimate local directions using the GED estimator as proposed in section IV.
3) Correct false estimated directions using the LMDC method as proposed in section V.
4) Interpolate red and blue channels using the CHI method.
5) Reduce color artefacts using the bilateral filter as proposed in section VI.

VIII. IMAGE QUALITY ASSESSMENT

Finding a consistent way to estimate image quality is a recurring problem in image processing. An important number of demosaicing algorithms are present in the literature and we need objective measures to quantify the performances of the different methods. It is generally agreed that current image measures cannot effectively quantify the perceptual quality of images obtained from a restoration or a reconstruction process [26]-[27]-[28].

Fig. 5. Results of different filters applied on the difference planes *R*. and *B*.

However, a global quantification can be obtained by combining subjective visual image quality assessments and the mean square error calculation between the original and the demosaiced image. Equation (7) shows the mean square error function, where *X* represents a set of *2-D* pixels positions, *v(x)* is the estimated pixel and *u(x)* is the original pixel at the *x* position. As proposes Li in [26], the measure's quantitative power can be improved by performing separate MSE calculations over edges on the one hand, and smooth regions on the other.

$$\Delta E = \frac{1}{N} \sum_{1 \le n \le N} \left\| u(x) - v(x) \right\| \tag{7}$$

In this section, we compare the image quality obtained with

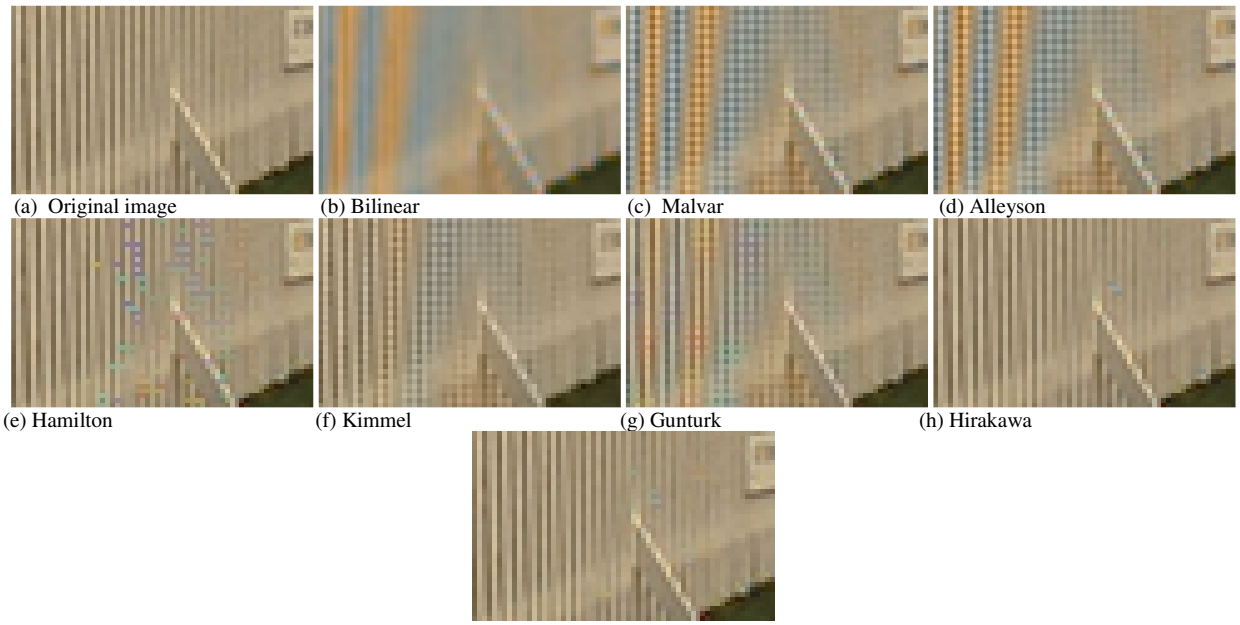

Fig. 6. Visual comparison of GEDI with common demosaicing algorithms.

our algorithm with that obtained using other demosaicing algorithms. For the comparison we use both the subjective criterion of visual appreciation, and the objective criterion of MSE calculation. The MSE is measured in both smooth and edge regions as well as in the overall image. We also measure the MSE in the red, green and blue plane separately. For the measure we use 24 reference images. These images were scanned at 3 color samples per pixel from film original. Color information is spatially sub-sampled to obtain images consisting of only one color per pixel, in agreement with the Bayer color filter arrangement.

A. Visual quality

Here we focus on the visual image subjective appreciation. We compare the demosaicing visual qualities of the different algorithms using the popular "lighthouse" image commonly referenced to evaluate demosaicing resolution. Fig. 6 shows the results produced by the implemented algorithms on a problematic image subset. We can see that GEDI produces comparable image quality to Hirakawa's method. Incorrect interpolation directions, moiré effects and color artifacts were almost completely absent. We compare also the image quality obtained with a real raw camera. For the experiments we used a consumer-level camera for which RAW data is available. We imaged a professional sharpness indicator target. Fig. 7 shows the results of different demosaicing algorithms on the same image subset. Fig. 7a is the original raw image. By looking at these results, we note that the bilinear interpolation completely erases the concentric circles visible on the original raw image. All algorithms results, except Hirakawa's and GEDI, induce moiré effects. The Hirakawa and Hamilton algorithms introduce incorrect direction interpolations. The Gunturk, Malvar, Alleyson and Kimmel methods also create zippering effects. GEDI clearly produces the better result. Moiré effects, incorrect interpolation direction choice and zippering effects appear completely absent.

B. Mean Square Error Calculation

In this section, we present the results of the mean square error average difference between the demosaiced images and the original images using a database of 24 reference images.

Table II shows the results of the MSE measure on smooth and edge regions and on the overall image. Looking at this table, we can observe that the GEDI algorithm yields MSE results very close to Hirakawa's. We can also note the good performances of the Gunturk algorithm. However, as we have seen before, this algorithm tends to induces color artifacts, moiré and zippering effects. Table III shows the results of the MSE measure on red, green and blue channels. As in table II this table highlights the good performances of our proposal. Fig. 8 shows the graphic results of the Table III.

In this section, we have shown that our demosaicing algorithm proposition outputs quality results at least equivalent to some of the best algorithms present in the literature. In the following section, we compare the algorithms computational complexity.

TABLE II
MEAN SQUARE ERROR CALCULATION ON EDGE REGIONS, SMOOTH REGIONS AND OVERALL IMAGE OVER 24 REFERENCE IMAGES

Algorithms	Edge regions	Smooth regions	Overall
Bilinear 3x3	168.06	23.07	47.86
Malvar	56.70	8.23	17.97
Alleyson	58.34	8.43	19.30
Kimmel	48.48	8.56	16.37
Hibbard	44.66	7.55	14.74
Hamilton	38.21	6.95	13.06
Hirakawa	31.53	5.90	11.34
GEDI	32.91	5.73	11.30
Gunturk	25.26	4.42	8.84

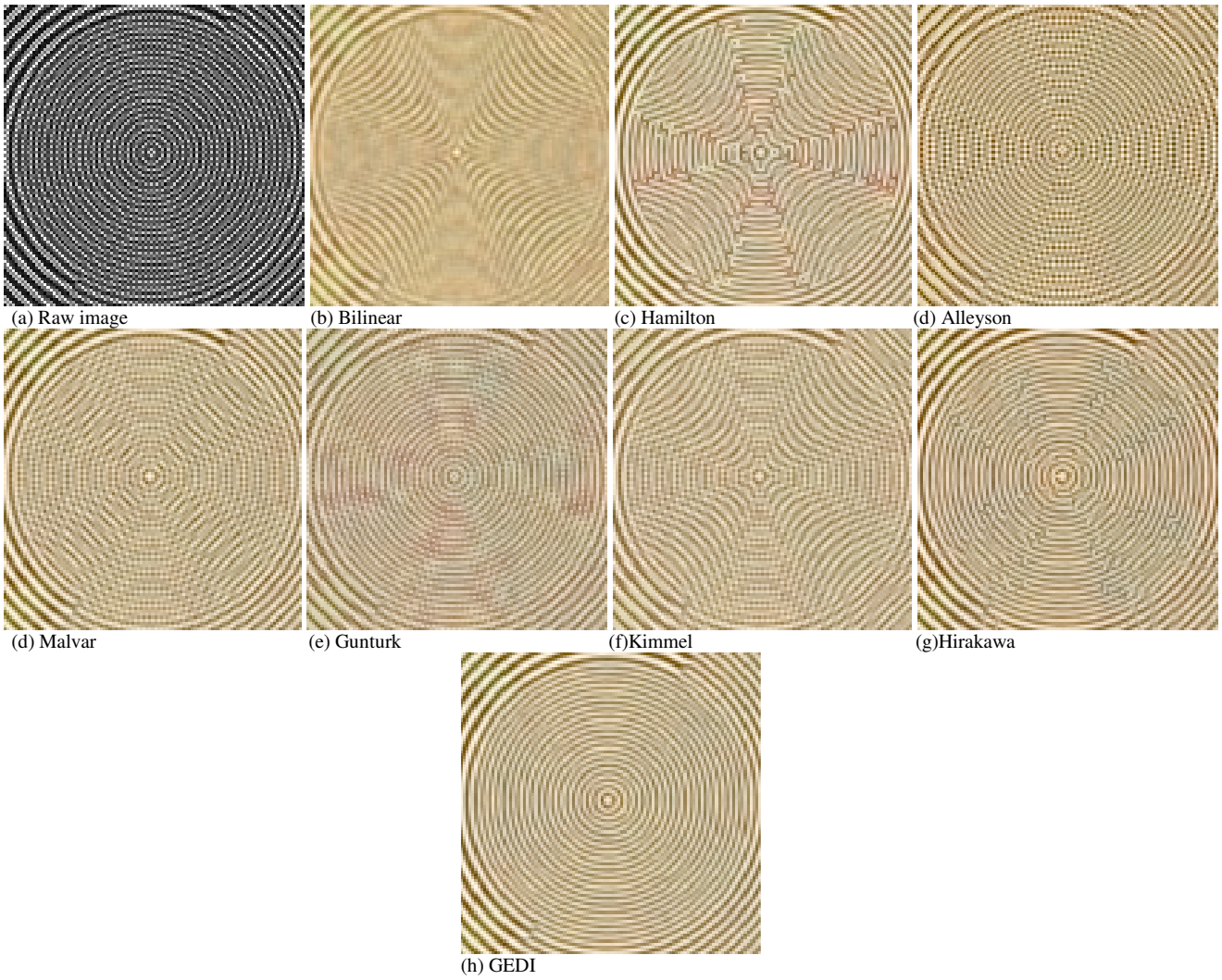

Fig. 7. Comparison of the visual quality obtained with different existing demosaicing methods.

TABLE III
MEAN SQUARE ERROR CALCULATION ON RED, GREEN AND BLUE CHANNELS OVER 24 REFERENCE IMAGES

Algorithms	Red channel	Green channel	Blue channel
Bilinear 3x3	44.25	52.23	47.11
Malvar	20.36	8.38	25.17
Alleyson	19.36	16.38	22.17
Kimmel	17.52	12.53	19.05
Hibbard	14	11.53	16.87
Hamilton	12.94	10.53	15.70
Hirakawa	11.96	8.07	14
GEDI	11.29	8.69	13.94
Gunturk	9.41	5.69	11.41

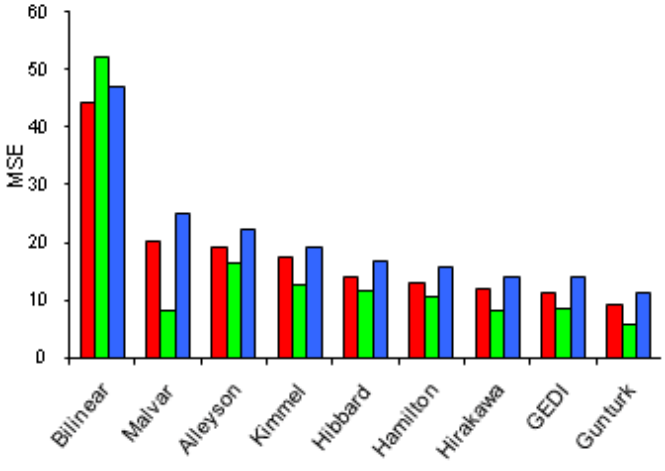

Fig. 8. MSE comparison on red, green and blue channels.

IX. COMPUTATIONAL COMPLEXITY

In this section, we compare the computational complexity of the demosaicing algorithms. Table IV shows the computational complexity of each studied algorithm by counting the number of operations per pixel. Fixed multiplication means multiplication by a fixed coefficient, which can be hard-coded with cumulative shift/adds. Table V shows the detailed counting of operations at each step the GEDI algorithm. In table IV, we can see that compared to Hirakawa and Gunturk, GEDI has a very low computational complexity comparable to the fastest algorithm such as Hamilton, Malvar, Alleyson and Bilinear. As we have shown in section VIII, this computational reduction is obtained without sacrificing image quality.

We conclude that our demosaicing algorithm proposal maintains or improves image quality while keeping computations low. In the following section we compare the performances of the GEDI, Hamilton and Hirakawa algorithm on a current DSP.

TABLE IV
ALGORITHMS COMPUTATIONAL COMPLEXITY COMPARISON

	multipli-cations	fixed multipli-cations	additions	Compa-risons	absolute values
Bilinear	0	4	3	0	0
Malvar	0	19	21	0	0
Alleyson	0	61	70	0	0
Kimmel	0	120	180	0	0
Hibbard	0	6	12	1	2
Hamilton	0	13/2	14	1	4
Hirakawa	24	24	88	71	12
GEDI	0	4	28	1	8
Gunturk	0	480	480	0	0

TABLE V
GEDI DETAILED COMPUTATIONAL COMPLEXITY

		fixed multipli-cation	ad-ditions	compari-sons	absolute values
Green	*Gv, Gh*	3	4	0	0
Interpolation	GED	0	14	1	8
LMDC	0	0	8	0	0
CHI	0	1	2	0	0
Total/pixel	0	4	28	1	8

X. SIMULATION AND COMPARISON ON DSP

We have implemented and simulated the Hamilton, Hirakawa and GEDI demosaicing algorithms on a typical mid-range media processor in use at the time of writing [29]. Each algorithm has been optimized (loop unrolling, separability, utilization of look up tables and custom DSP operation). A complete optimization procedure of the Hirakawa algorithm dedicated to the chosen processor is described in [30]. For the simulations we consider VGA resolution, a typical video resolution in embedded camera. The results are shown in section IX-B.

The simulations were done with images at VGA resolution using a processor running at 350MHz clock frequency. In Fig. 9 we can see the results of the simulation given in frames per second (fps). We can see that Hamilton and GEDI can be run on VGA video sequences at over 25 frames per second (fps). We also note that with 50.54 fps GEDI runs 1/3 as slow as Hamilton (74.73 fps). We observe that Hirakawa cannot process videos at VGA resolution, as it only runs at 7.64 fps. These results show that by using the GEDI algorithm it is possible to improve image quality demosacing while keeping real time processing on embedded multimedia devices.

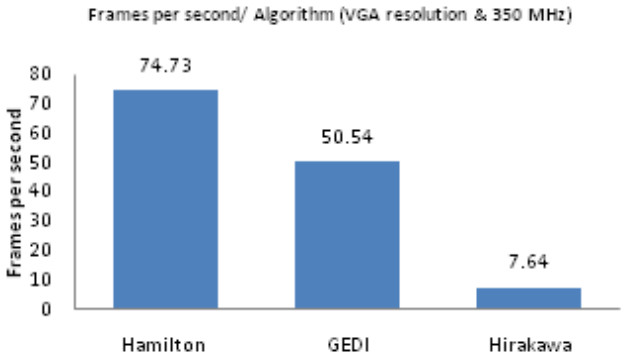

Fig. 9. Frame per second comparison computing for a VGA resolution image on a current DSP.

XI. CONCLUSION

In this paper, a green edge directed demosaicing algorithm was presented. We propose a novel estimator wich we name GED to estimate local details directions, using gradient measures in the vertical and the horizontal interpolated green channel. We developed an improved a method to detect and correct false interpolation directions, wich we call LMDC. We showed that bilateral filtering provided better results than gradient on the R_{-} and B_{-} difference channels to suppress color artifacts. Experimental data demonstrates the good performances of our algorithm. We also exhibited the real time performance of our algorithm on a typical current multimedia processor.

REFERENCES

[1] B.E.Bayer, *Color Imaging Array*. United State Patent, 3,971,065, 1976.

[2] D.Alleyson, "30 ans de demosaicage - 30 years of demosaicing," *GRETSI 2004*, vol. 21, pp. 561–581, 2004.

[3] B.K.Gunturk, J.Glotzbach, Y. Altunbasak, R.W.Schafer, and R. M.Mersereau, "Demosaicking: Color filter array interpolation," *IEEE Signal processing magazine*, vol. 22, pp. 44–54, 2005.

[4] H.J.Trussel and R.E.Hartwing, "Mathematics for demosaicking," *IEEE Transactions on image processing*, vol. 11, pp. 485–492, 2002.

[5] R.Costantini and S.Susstrunk, "Virtual sensor design," *Proc. IS&T/SPIE Electronic Imaging 2004: Sensors and Camera Systems for Scientific, Industrial, and Digital Photography Applications*, vol. 5301, pp. 408–419, 2004.

[6] D.R.Cock, "Single-chip electronic color camera with color dependent birefringent optical spatial frequency filter and red and blue signal signal interpolating circuit," *United States Patent number 4,605,956*, 1986.

[7] R. Kimmel, "Demosaicing: image reconstruction from color ccd samples," *Image Processing, IEEE Transactions on*, vol. 8, no. 9, pp. 1221–1228, 1999.

[8] K.Hirakawa and T.Parks, "Adaptive homogeneity-directed demosaicing algorithm," *Image Processing, IEEE Transactions on*, vol. 14, pp. 360–369, 2005.

[9] R.H.Hibbard, *Apparatus and method for adaptively interpolating a full color image utilizing luminance gradient*. us patent 5,382,976 to Eastman

Kodak Compagny, Patent and Trademark office, Washington, 1995.
[10] D.R.Cock, "Reconstruction of ccd images using template matching," *IS&T's 47th Annual Conference / ICPS*, pp. 380–385, 1994.
[11] J.A.Weldy, "Optimized design for a single-sensor color electronic camera system," *Proc. SPIE*, vol. 1071, pp. 300–307, 1988.
[12] J.E.Adams, "Interactions between color plane interpolation and other image processing functions in electronic photography," *Proc. SPIE*, vol. 2416, pp. 144–151, 1995.
[13] W.T.Freeman, *Method and apparatus for reconstructing missing color samples*. us patent 4,774,565 to Polaroid Corporation, Cambridge, Mass, 1988.
[14] S.C.Pei and I.K.Tam, "Effective color interpolation in ccd color filter array using signal correlation," *IEEE Trans. Circuits Syst. Video Technol.*, vol. 13, pp. 503–513, 2003.
[15] H.D.Crane, J. Peter, and E.Martinez-Uriegas, "Method and apparatus for decoding spatiochromatically multiplexed color images using predetermined coefficients," *US patent 5,901,242 to SRI International, Patent and Trademark Office Washington D.C*, 1999.
[16] H.S.Malvar, L. He, and Y.Yacobi, "High-quality linear interpolation for demosaicing of bayer-patterned color images," *IEEE International Conference on Acoustics, Speech, and Signal Processing*, 2004.
[17] C.Tomasi and R.Manduchi, "Bilateral filtering for gray and color images," pp. 839–846, 1998.
[18] R.Ramanath and W.E.Snyder, "Adaptive demosaicking," *Journal of Electronic Imaging*, vol. 12, no. 4, pp. 633–642, 2003.
[19] C.A.Laroche and M.A.Prescott, *Apparatus and method for adaptively interpolating a full color image utilizing chrominance gradient*. us patent 5,373,322 to Eastman Kodak Compagny, Patent and Trademark office, Washington, 1994.
[20] J.F.Hamilton and J.E.Adams, *Adaptive color plan interpolation in single sensor color electronic camera*. US Patent 5,629,734 to Eastman Kodak Compagny, Patent and Trademark office, Washington, 1997.
[21] D.Alleyson, S.Süstrunk, and J.Herault, "Color demosaicing by estimating luminance and opponent chromatic signals in the fourrier domain," *Proc. Color Imaging Conf: Color Science, Systems, Applications*, pp. 331–336, 2002.
[22] B.K.Gunturk, Y.Altunbasak, and R.M.Mesereau, "Color plane interpolation using alternating projections," *IEEE transactions on image processing*, vol. 11, pp. 997–1013, 2002.
[23] J.W.Glotzbach, R.W.Schafer, and K.Illgner, "A method of color filter array interpolation with alias cancellation properties," *IEEE International Conference on Image Processing*, pp. 141–144, 2001.
[24] D.Taubman, "Generalized wiener reconstruction of images from colour sensor data using a scale invariant prior," *International conference on image processing*, vol. 3, pp. 801–804, 2000.
[25] W.T.Freeman, *Median filter for reconstructing missing color samples*. US Patent 4,724,395, to Polaroid Corporation, Patent and Trademark Office, Washington, D.C., 1988.
[26] X.Li and M.T.Orchard, "New edge-directed interpolation," *IEEE transaction on Image Processing*, vol. 10, 2001.
[27] Z.Wang, A.C.Bovik, and L.Lu, "Why is image quality assesment so difficult," *IEEE international conference on Acoustics, Speech, Signal Processing*, vol. 4, 2002.
[28] B.Girod, "What's wrong with mean-squarred error," *Digital Images and Human Vision, A.A. Watson, Ed Cambridge, MA: MIT Press*, 1993.
[29] J.W.VanDeWaerdt, S. Vassiliadis, S. Das, S. Mirolo, C. Yen, B. Zhong, C. Basto, J.-P. van Itegem, D. Amirtharaj, K. Kalra, P. Rodriguez, and H. van Antwerpen, "The tm3270 media-processor," pp. 331–342, 2005.
[30] H.Phelippeau, M.Akil, T.Fraga, S.Bara, and H.Talbot, "Demosaicing on trimedia 3270," *European Workshop on Design and Architectures for Signal and Image Processing*, 2007.

Harold Phelippeau received the M.S. degree in optoelectronic, signal and image engineering from Université d'Angers (France) in 2006 and his PhD. from Université de Paris-Est, in 2009. His interests include single camera image processing for multimedia mobile applications.

Hugues Talbot (M '2005) graduated from Ecole Centrale de Paris in 1989 and got his PhD. from Ecole des Mines de Paris in 1993. He worked at the CSIRO in Australia 1994-2004 and is now an associate professor at Université Paris-Est. His interests include image filtering and segmentation, mathematical morphology and optimization. He has published more than 50 research papers in these areas. He was awarded the 2006 DuPont and several other awards for his work on automated melanoma diagnosis.

Mohamed Akil received his phd degree from the Montpellier university (France) in 1981 and his doctorat d'état from the Pierre et Marie curie University (Paris, France) in 1985. He currently teaches and does research with the position of Professor at computer science department, ESIEE, Paris. He is a member of Institut Gaspard-Monge, unite mixte de recherche CNRS-UMLPE-ESIEE, UMR 8049. His research interests are Architecture for image processing, Image compression, Reconfigurable architecture and FPGA, High-level Design Methodology for multi-FPGA, mixed architecture (DSP/FPGA) and System on Chip (SoC). Dr. Akil has more than 80 research papers in the above areas.

Stefan Bara received the M.S. degree in electrical and computer engineering from Polytechnic University of Bucarest, Romania, in 1996 and the PhD. degree in microelectronic from Institut National Polytechnique of Grenoble, France, in 2000.His interests include image processing for mobile applications.